Journal of Energy Storage 56 (2022) 105831

Contents lists available at ScienceDirect

Journal of Energy Storage

journal homepage: www.elsevier.com/locate/est

Research papers

Modified extended Kalman filtering algorithm for precise voltage and state-of-charge estimations of rechargeable batteries

Fan Yang [a,1], Dongliang Shi [a,1], Kwok-ho Lam [a,b,*,**]

[a] Department of Electrical Engineering, The Hong Kong Polytechnic University, Hong Kong, China
[b] Centre for Medical and Industrial Ultrasonics, James Watt School of Engineering, University of Glasgow, Glasgow, Scotland, UK

ARTICLE INFO

Keywords:
Modified EKF algorithm
Extended Kalman filtering
State-of-charge
Electric vehicle
Lithium-ion battery

ABSTRACT

With the popularization of electric vehicles (EVs), the voltage and state-of-charge (*SOC*) estimations of rechargeable batteries are of great significance. The *SOC* parameter has been used as an indicator for delivering the electrical energy of rechargeable lithium-ion batteries (LIBs), while the voltage has been a critical parameter needed to monitor to prevent the cause of battery damage especially during the charging and discharging process. Thus, the research focus is to estimate the *SOC* and voltage accurately using algorithms. With the capability of avoiding major estimation errors, conventional extended Kalman Filtering (EKF) has been employed to estimate the optimal value of *SOC* using the parameters obtained by indirect measurements, such as voltage and current. However, the algorithm suffers from limited precision in *SOC* and voltage estimations, and there is still no in-depth investigation of the error reduction in voltage prediction. Although the *SOC* accuracy can be improved by a joint algorithm such as double Kalman filtering, optimization of EKF itself is still needed due to the superposition of nonlinear errors. This study reveals that the conventional EKF algorithm induces estimation errors especially when the current abruptly changes. In this study, the research on the modified extended Kalman filtering (MEKF) algorithm was conducted for estimating the voltage and *SOC* of the LIBs with great improvement in estimation accuracy. The YUASA LEV50 cell was subjected to a standard discharging rate of 0.2C at 298 K to acquire offline parameters, followed with the newly proposed dynamic estimation mathematical battery model (DBOFT) for the optimization of estimations. This is the first time to propose a method of combining gain matrix and noise to reduce the error of voltage estimation at the current turning points, which greatly improves the accuracy of voltage estimation. Specifically, the MEKF algorithm is capable of adjusting the parameters in real-time and reducing the *SOC* estimation error. The *SOC* error estimated by the MEKF algorithm was reduced to 0.0052 % under the current rate of 0.2C. Finally, the maximum estimated voltage error was reduced to 0.972 % while the *SOC* estimation error was reduced to 0.01016 % under the same working current. The precise voltage and *SOC* estimations obtained by the MEKF with higher accuracy than traditional methods were validated under experimental verification, which is crucial for the life extension of LIBs and the safety of the battery management system (BMS).

1. Introduction

The environmental pollution caused by traditional automobile energy is becoming serious, which is accompanied by the issue of an energy crisis [1]. Up to now, many countries have developed various technologies to slow down global warming [1]. As electric vehicles (EVs) have the potential to reduce CO_2 emissions to a certain extent, corresponding technologies have been developed rapidly [2]. Thus, the critical part of EVs, a battery management system (BMS), has been widely concerned. An accurate estimation of the state-of-charge (*SOC*) of the battery in BMS can enhance the power delivery performance of the battery system, improve the safety of the battery, prevent overcharge and over-discharge of the battery, prolong the service life of the battery, and optimize the distribution of energy in the system [3]. Up to now, the *SOC* of the battery is defined as the energy currently stored in the battery, but there is no uniform standard method for calculation or estimation [3].

* Corresponding author at: Department of Electrical Engineering, The Hong Kong Polytechnic University, Hong Kong, China.
** Corresponding author at: Centre for Medical and Industrial Ultrasonics, James Watt School of Engineering, University of Glasgow, Glasgow, Scotland, UK.
E-mail addresses: 21118694r@connect.polyu.hk (F. Yang), Kwokho.Lam@glasgow.ac.uk (K.-h. Lam).
[1] Equally contributed.

https://doi.org/10.1016/j.est.2022.105831
Received 9 June 2022; Received in revised form 1 October 2022; Accepted 3 October 2022
Available online 21 October 2022

Nomenclature

AEKF	Adaptive extended Kalman filter
Ah	Ampere-hour
BMS	Battery management system
DEKF	Dual extended Kalman filter
DBOFT	Dynamic best-fitting order tracking
EKF	Extended Kalman filter
EV	Electrical vehicle
LIB	Lithium-ion battery
MEKF	Modified extended Kalman filter
OCV	Open-circuit voltage
EM	Electrochemical Model
ECM	Equivalent Circuit Model

SOC was proposed as a key indicator in battery monitoring through the open-circuit voltage (OCV) method for electric wheelchairs in 1992 [4]. However, the measured voltage cannot describe the variations of internal battery parameters induced by many external factors, resulting in a large error in the estimated *SOC*. Then, the *SOC* estimation algorithm of lead-acid batteries based on an accurate battery model was developed in 2001 to minimize the error during the charging and discharging process [5]. With the introduction of the battery model, the *SOC* estimation error caused by the change of internal battery parameters can be reduced through the correlation methods by measuring the voltage and current of the battery directly, the OCV method, and the ampere-hour (Ah) integral method [2]. In recent years, intelligent algorithms such as Kalman filter and neural network have attracted attention, developed and optimized for improving the accuracy of *SOC* estimation [6–8]. Moreover, intelligent algorithms have further been used in battery model building and capacity estimation to enhance the reliability and accuracy of battery monitoring. The joint algorithm combining several intelligent algorithms for *SOC* estimation has gradually become a research trend [9]. Meanwhile, in order to reduce the error caused by the inconsistencies in battery packs, a data-driven method based on the black-box model was proposed to estimate the *SOC* [10,11]. Nevertheless, the black-box model still has the disadvantages of obtaining insufficient training data and difficulty to be widely applied in practice [10].

Currently, the approaches for *SOC* estimation can be classified as the following due to the different focuses in the research process: (1) Model-based *SOC* estimation; (2) Sensor-based *SOC* estimation; and (3) Algorithm-based *SOC* estimation.

(1) Model-based *SOC* estimation

Model-based estimation is classified into three different types including the electrochemical model (EM), equivalent circuit model (ECM), and black-box model. The estimation of battery *SOC* based on the EM and ECM needs to combine with other estimation approaches such as OCV and Ah methods, which is not necessary for the black-box model [7,11]. The EM can describe the chemical processes of the battery with great details for *SOC* estimation, however, it is not user-friendly due to the complexity of parameter setting and the initial salt concentration in the overall heat capacity [12]. The ECM model estimates the battery *SOC* through the resistance, capacitance, and voltage characteristics, which is relatively simple to build, but lacks accuracy when describing the changes of internal battery parameters [13]. The black-box model was developed with the advancement of computing technology, which can be used as a data-driven method to estimate the battery *SOC*. The black-box modeling methods are divided into fuzzy-based estimation, fuzzy-based neural network, bio-inspired algorithm, and support vector machines [7]. Although the black-box model can reduce the *SOC* estimation error induced by the inconsistency issue in battery packs, it is still difficult to obtain a large amount of data and realize the real applications through training [10,14].

(2) Sensor-based *SOC* estimation

Sensor-based *SOC* estimation approach is an emerging research topic, which can simultaneously realize both *SOC* estimation and internal damage monitoring of batteries without the involvement of voltage and current data [15,16]. The representative approach of sensor-based *SOC* estimation is to use the ultrasonic transducer to monitor the battery in real-time, and to estimate *SOC* by analyzing the relationship between the ultrasonic signal and *SOC* [16]. The sensor-based *SOC* estimation methods can achieve the detection on both internal and external damages of the battery during the battery *SOC* estimation, but the *SOC* estimation error obtained by the sensor calculation is relatively large.

(3) Algorithm-based *SOC* estimation

Algorithm-based methods are widely used to estimate the *SOC*, such as the OCV method and the Ah integral method. The drawback origins from the difficulty of automatic determination of the initial value of *SOC*, resulting in a large cumulative error [2,17].

To enhance the estimation accuracy, the application of the intelligent algorithm is essential, such as the neural network method and the Kalman filtering method [18,19]. The neural network method relies on a large number of samples for data training to achieve high accuracy [19]. However, this method is very sensitive to the training data and training methods [19]. The Kalman filtering method obtains the minimum variance estimation by a recursive algorithm according to the collected voltage and current [18,20]. Thus, this method exhibits the merits of avoiding inaccurate estimation of the initial value of *SOC* and eliminating cumulative error [20]. Nevertheless, the accuracy of *SOC* estimation would be limited if the method is used to model batteries because the conventional Kalman filtering algorithm is only suitable for linear systems [20].

G. L. Plett firstly proposed that the EKF can be applied to *SOC* estimation in a BMS of LiPB-based HEV battery packs, which was experimentally proven to be feasible. However, the error in *SOC* estimation for this preliminary EKF method was higher than 5 % [6,21]. Subsequently, researchers introduced various approaches to improve the accuracy of *SOC* estimation by EKF. For example, A. Vasebi et al. reduced the error of *SOC* estimation to 2 % using the EKF by adopting a novel model based on RC and hysteresis battery models, but the voltage error was as high as 30 % under irregular current discharge tests [22]. Joint algorithms such as the dual EKF (DEKF) method, and the online parameter identification approach were adopted for the real-time monitoring of battery parameters [23]. For example, L. Xia et al. achieved low errors of 1.83 % and 1.92 % in state-of-energy and *SOC* estimations, respectively, at different working temperatures and conditions through the approaches of online parameter identification and DEKF [24]. Though H. Dai et al. also successfully reduced the maximum *SOC* error to 3 %, the superposition of non-linear errors caused by the introduction of other algorithms led to more unstable *SOC* and voltage estimations [25,26]. Researchers have also tried to reduce the *SOC* error by improving the EKF algorithm structure, for instance, H. He et al. improved the *SOC* accuracy using a filter divergence judgment condition, which could reduce the *SOC* estimation error to 2.94 %, but the voltage estimation error was up to 35 % [27]. Besides, novel intelligent EKF-based algorithms have been investigated, for example, M. Dahmardeh et al. adopted the integration of EKF and an uncertainty quantification method to acquire reliable battery *SOC* estimation without involving a specific battery model, which was a new attempt for battery *SOC* estimation and of great importance for intelligent estimation [28]. The current sensor-free approach for *SOC* and current co-estimation was developed by

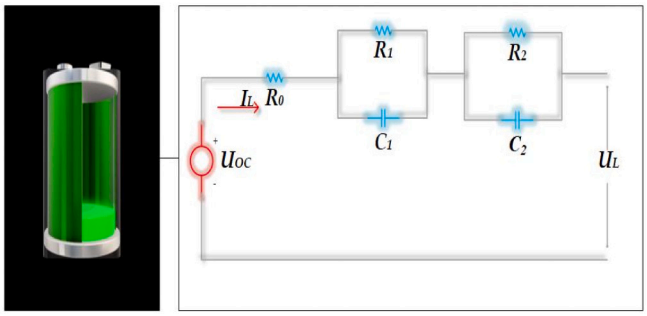

Fig. 1. The second-order RC equivalent circuit battery model of a LIB.

Zhongbao Wei, which is a novel perspective to ease the burden of the instrument [29]. Intelligent algorithms such as machine learning have also been used to resolve the issues of economic emission dispatch in power systems, which is crucial for improving the power system management and environmental pollution issues. L. Li et al. proposed the improved tunicate swarm algorithm (ITSA) and validated successfully for achieving much precise dispatch strategy [30]. Z. Liu solved the hybrid dynamic economic emission dispatch (HDEED) by proposing a moth-flame optimization algorithm based on position disturbance updating strategy (MFO_PDU), which could make the fuel cost less than HHO, TSA and MFO algorithms, and is beneficial for reducing the pollutant emission [31].

In summary, the optimization of intelligent algorithms to improve the accuracy of *SOC* estimation is still the main research focus in the future, and the research gaps for the intelligent EKF algorithms can be concluded as follows: (1) The existing research reduced the error of voltage estimation by improving the battery model, however, there is no in-depth research on how to reduce the error of the voltage estimation at the current changing points. (2) Although matrix conditioning techniques have been applied to the improvement of adaptive EKF, no research work has been done on combining matrix conditioning techniques with the Kalman gain to accelerate the convergence and thus reduce the error of the EKF algorithm. (3) Various approaches have been used to improve the accuracy of *SOC* estimation by EKF, however, the incremental study to reduce the error of *SOC* estimation by improving the voltage estimation has not been explored. Consequently, more accurate *SOC* estimation and voltage estimation have been the sought-after goal all the time.

Aiming at the research gaps, the contributions of this research can be summarized as follows: (1) During the operation of the EKF algorithm, the burst of estimated voltage error at the point of current changing is investigated in depth for the first time and improved effectively based on the noise adjustment technique. (2) The dynamic best-fitting order tracking (DBOFT) model is proposed and implemented based on the second-order RC equivalent circuit battery model through the matrix adjustment technique in order to reduce the distinct error that existed in the process of linearization of the nonlinear system. This was also validated to be effective for the accuracy improvement of *SOC* estimation. (3) The EKF algorithm is further modified to enhance the accuracy of the voltage and *SOC* estimations by investigating the relationships between the Kalman gain, and the *SOC* and voltage estimation error specifically when the current changes, which can be used to improve the estimation accuracy by matrix and noise conditioning techniques. In this work, the newly developed modified extended Kalman filtering (MEKF) algorithm was verified with experiments using LIBs. The verification showed that our proposed algorithm significantly improved the accuracy of both voltage and *SOC* estimations of batteries.

In this paper, Section 2 introduces the principle of the mathematical model of DBOFT based on the second-order RC equivalent circuit, and the structure of DBOFT. Section 3 proposes the MEKF algorithm based on matrix adjustment technology and DBOFT. Section 4 verifies the accuracy of the DBOFT model experimentally and demonstrates the feasibility of the MEKF by charging and discharging batteries of various capacities at different discharging rates. Section 5 summarizes the research work and provides a prospect for future work.

2. The dynamic estimated mathematical battery model

Taking into account the efficiency of the algorithm and the computational burden, the second-order RC equivalent circuit model was applied because it is much more precise than the first-order one but shows no big difference from the third-order one. The symbolic representation of the proposed model for a LIB is shown in Fig. 1, where the internal resistance of the battery is divided into ohmic internal resistance, R_0, and polarization internal resistances, R_1 and R_2, respectively. The R_0 is composed of the resistances of electrode material, electrolyte, and diaphragm [32]. The R_1 and R_2 refer to the resistance caused by polarization during an electrochemical reaction [32]. The U_{OC} is the OCV of the battery. The parallel connected R_1 and C_1 represent the polarization process of electrochemical reaction with a small time-constant; and the R_2 and C_2 emulate the polarization process of electrochemical reaction with a large time-constant. U_L correlates to the terminal voltage of the battery, and I_L stands for the load current.

The second-order RC equivalent battery model is considered an accurate mathematical algorithm for battery modeling [33]. Nevertheless, the accuracy of the mathematical model in the algorithm varies against the order of the fitting formula which would affect the trend of the fitting curve as well as the estimated battery parameters at specific moments. Thus, the higher fitting order may not improve the accuracy of the battery model. On the contrary, the high fitting order would greatly

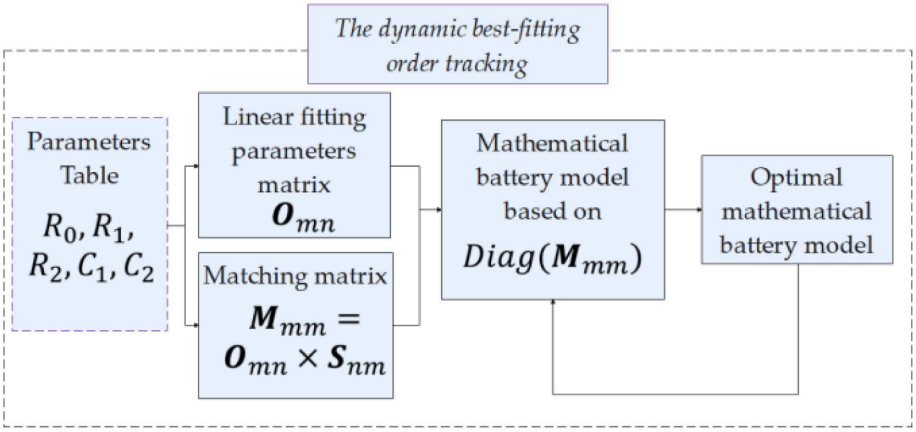

Fig. 2. The block diagram of dynamic best-fitting order tracking (DBOFT) mechanism.

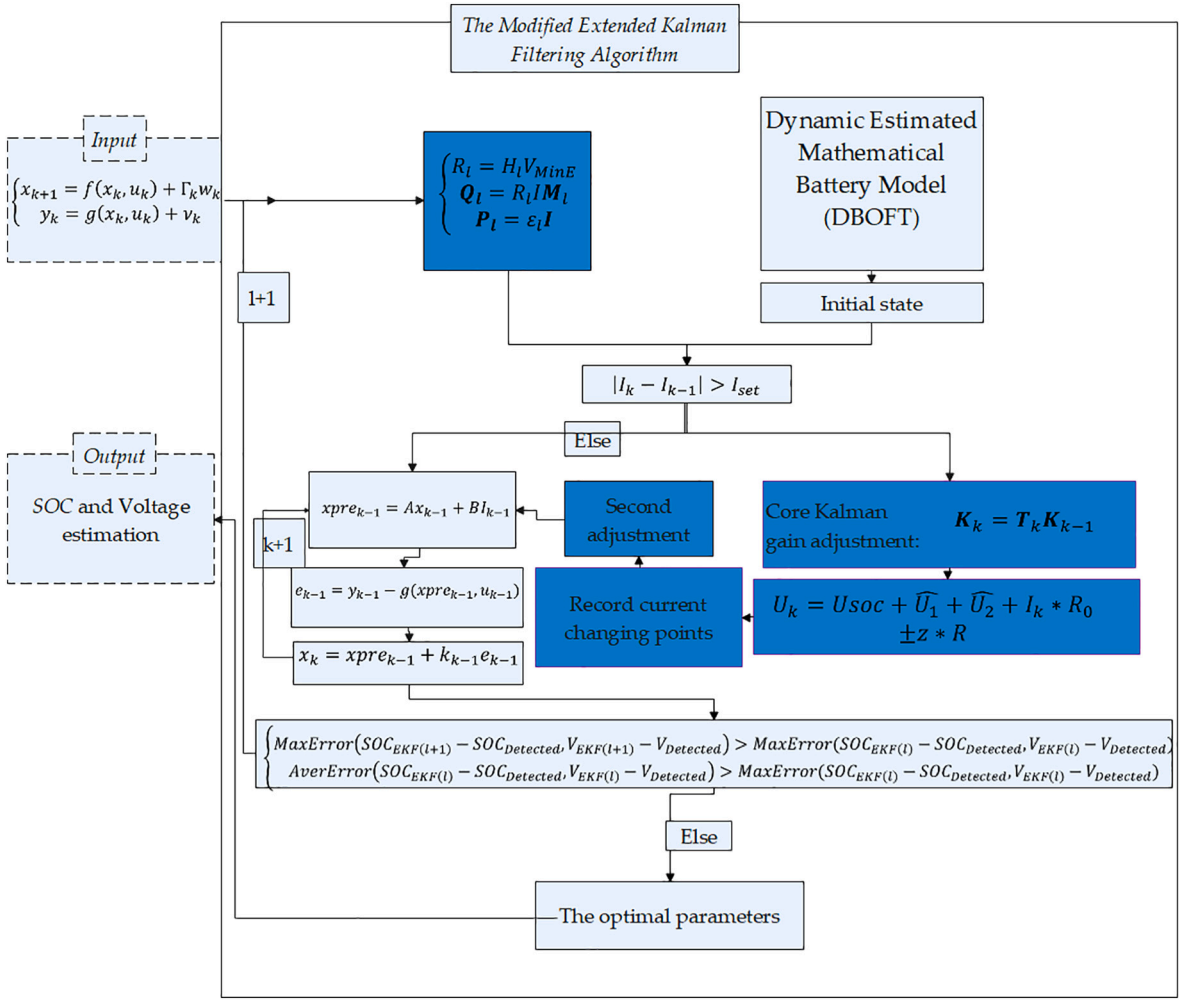

Fig. 3. The MEKF algorithm with DBOFT.

Table 1
The offline parameters of YUASA LEV50 cell.

SOC	OCV(V)	R_0 (Ω)	R_1 (Ω)	C_1 (F)	R_2 (Ω)	C_2 (F)
0.9	4.050	0.003	0.532	2.7E+0	0.0011	180,765
0.8	4.017	0.003	0.528	4.1E+06	0.0007	291,760
0.7	3.99	0.004	0.525	3.6E+06	0.0008	262,716
0.6	3.967	0.004	0.521	2.5E+06	0.0011	264,112
0.5	3.926	0.004	0.516	2.2E+06	0.00099	272,156
0.4	3.878	0.004	0.510	2.6E+06	0.00081	277,435
0.3	3.814	0.004	0.501	2.4E+06	0.00076	250,739
0.2	3.77	0.004	0.495	2.6E+06	0.00085	255,439
0.1	3.67	0.004	0.481	1.1E+06	0.0011	245,458
0	3.36	0.007	0.432	0.7E+06	0.0097	15.963

increase the complexity of the algorithm if all the battery parameters at each moment are identified for operation. Without considering the influence of the battery parameter identification method, the dynamic best-fitting order tracking (DBOFT) is proposed and implemented based on the RC equivalent circuit battery model to automatically determine the optimal fitting order. The idea is to use matrix matching combined with algorithm feedback to achieve the purpose.

Fig. 2 shows the block diagram of DBOFT. The parameters table contains the parameters such as R_0, R_1, R_2, C_1, C_2, which are identified by the offline parameter identification method. Then the polynomial fitting parameters P_n in the matrix $\boldsymbol{O}_{mn}$can be obtained by different order polynomial fittings. $\boldsymbol{S}_{nm}$ is the essential component consisting of *SOC*. The expressions of $\boldsymbol{O}_{mn}$, $\boldsymbol{S}_{nm}$ and $Diag(\boldsymbol{M}_{mm})$ are as follows:

$$\boldsymbol{O}_{mn} = \begin{bmatrix} V_1 & \cdots & V_n \\ \vdots & \ddots & \vdots \\ 0 & \cdots & V_{n-m+1} \end{bmatrix} \tag{1}$$

$$\boldsymbol{S}_{nm} = \begin{bmatrix} SOC^{n-1} & \cdots & 0 \\ \vdots & \ddots & \vdots \\ 1 & 1 & 1 \end{bmatrix} \tag{2}$$

$$Diag(\boldsymbol{M}_{mm}) = V_n SOC^{n-1} + V_{n-1} SOC^{n-2} + \ldots + V_1 \tag{3}$$

A mathematical model that best matches the external characteristics of the LIBs is iteratively filtered through DBOFT and then applied to the voltage and *SOC* estimations.

3. The modified EKF (MEKF) algorithm

3.1. The voltage estimation

Though the extended Kalman filtering (EKF) method is commonly used to estimate the *SOC* of LIBs, which can also estimate the voltage during the iteration process [34], apparent errors still exist because of the following three major issues: (1) the voltage estimation error occurs in the process of the EKF algorithm, which is mainly caused by the battery model [32]; (2) the *SOC* estimation sometimes fails to converge such that the error increases with the processed data [35]; (3) the accuracy of *SOC* and voltage estimations is highly influenced by various noises such as unknown system noise and observation noise [20].

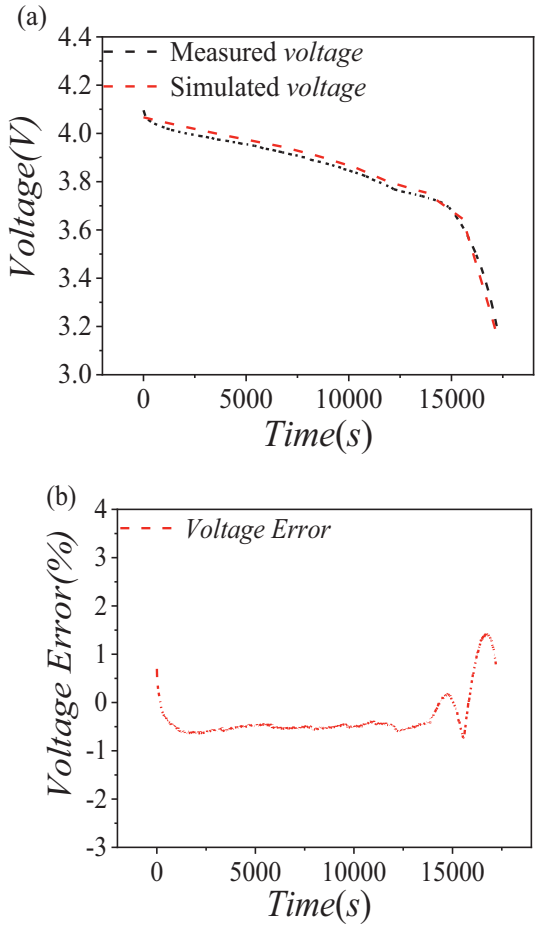

Fig. 4. (**a**) Comparison between measured and simulated voltages; and (**b**) the corresponding error as a function of discharging time.

Researchers improved the EKF algorithm in different ways for reducing voltage and *SOC* estimation errors. The battery model used in the EKF algorithm was shown to affect the accuracy of voltage and *SOC* estimations [32]. The Thevenin model with the covariance matrix matching technique could reduce the estimated voltage and *SOC* errors to 1 % and 2 %, respectively [36]. The EKF method with a partnership for the new generation of vehicle (PNGV) battery model was shown to reduce the *SOC* error to 2.78 % [37]. By adopting a two-order equivalent circuit model with an improved parameter identification, the average *SOC* estimation error could be reduced to 1.39 % [38]. Besides, as noise exists in the EKF process, the noise adaption combined with the improved parameter identification could further reduce the maximal *SOC* error to 2.94 % [39].

Though the errors were shown to reduce using different approaches with the EKF method, the estimated voltage error increased along with the variation of current. Thus, the EKF algorithm is modified for solving the aforementioned issue. This is the first time to propose detecting the varied current points to reduce the estimation errors of voltage and *SOC* simultaneously based on the modified EKF (MEKF) algorithm. The DBOFT in Section 2 is specifically designed for the mathematical calculation of battery simulation in the MEKF algorithm, which can be adapted to the equivalent circuit battery model with different RC orders.

Fig. 3 shows the block diagram of the MEKF algorithm in which the modifications mainly aim at reducing the voltage estimation error induced by the variation of the electric current of the battery. The MEKF algorithm specifically uses matrix matching and noise adjustment techniques to reduce the voltage estimation error at the turning points of current, which is based on the principle that the estimated values are

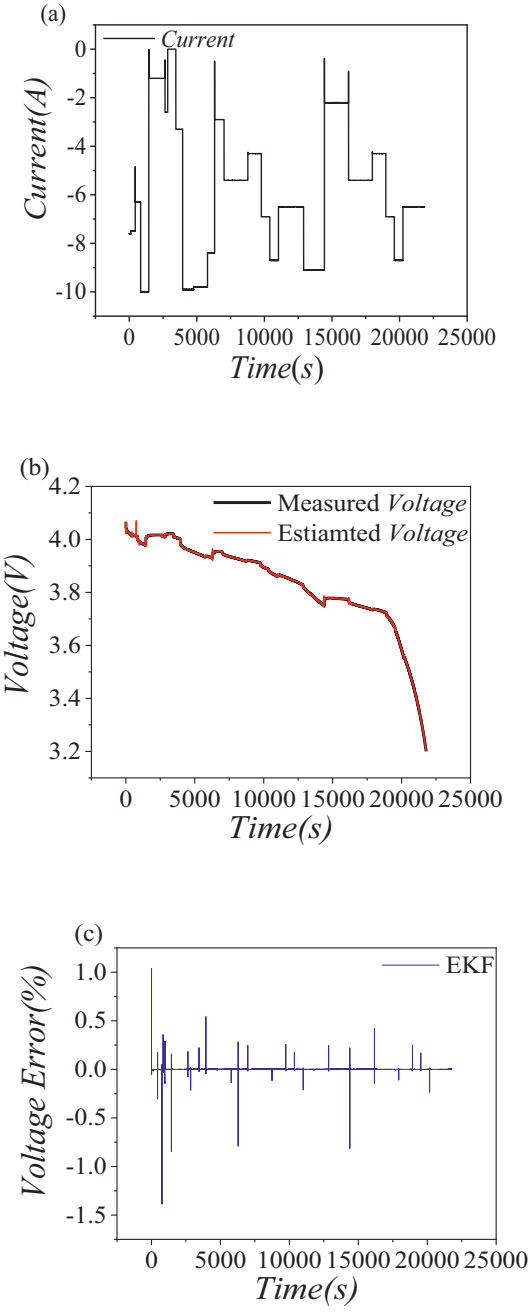

Fig. 5. (a) The irregular current applied to the battery, (b) the comparison of experimental and estimated voltages using the EKF method, and (c) the corresponding error.

kept corrected by changing the Kalman gain in the calculation of the EKF method [40]. However, it takes time to make corrections using the self-convergence process of the algorithm, resulting in a large voltage estimation error at the turning point of the current. In this study, Eq. (4) is designed for the Kalman gain adjustment while Eq. (5) is designed for the voltage estimation adjustment. $\boldsymbol{T}_k$ is the diagonal matrix for the adjustment of Kalman gain, and z is the adjustment parameter that depends on the maximum voltage estimation error.

$$\boldsymbol{K}_k = \boldsymbol{T}_k \boldsymbol{K}_{k-1} \tag{4}$$

$$U_k = Usoc + \widehat{U}_1 + \widehat{U}_2 + I_k{}^*R_0 \pm z^*R \tag{5}$$

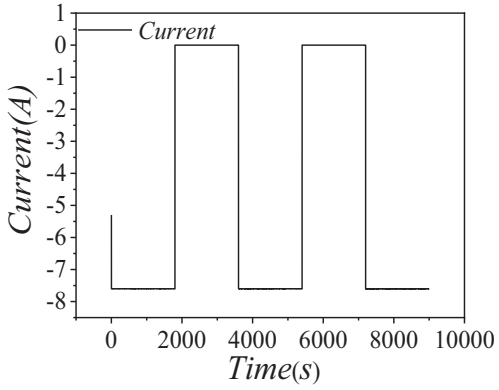

Fig. 6. The periodic current is applied to the battery.

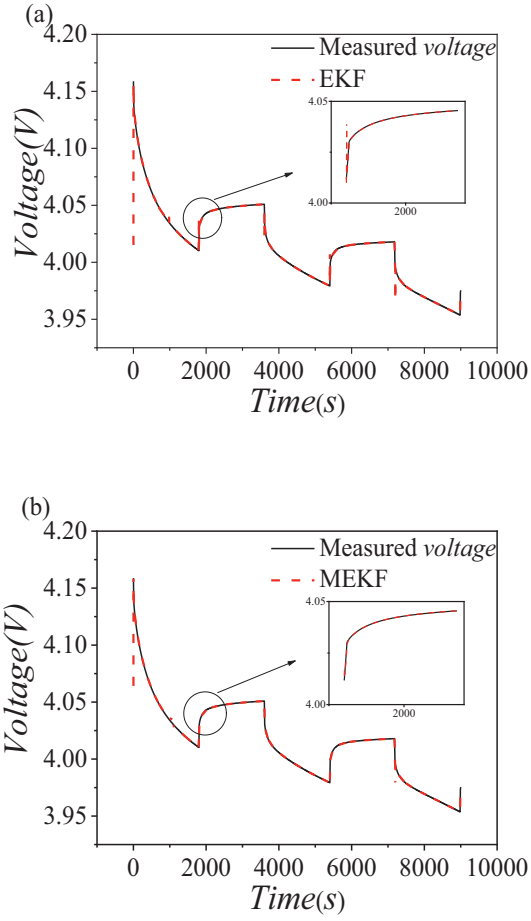

Fig. 7. Comparison of measured and estimated voltages using the (a) EKF and (b) MEKF algorithms.

3.2. The SOC estimation

Kalman filter is an algorithm that can obtain the best estimation for the linear system with the smallest variance [41]. Extended Kalman Filtering (EKF) algorithm is a method based on a Kalman filter that optimizes the estimation of non-linear systems [42]. According to the Kalman filtering algorithm, the linear discrete system equation can be expressed as follow:

$$x_{k+1} = \boldsymbol{A}_{\mathbf{k}} x_k + \boldsymbol{B}_{\mathbf{k}} u_{k+} w_k \tag{6}$$

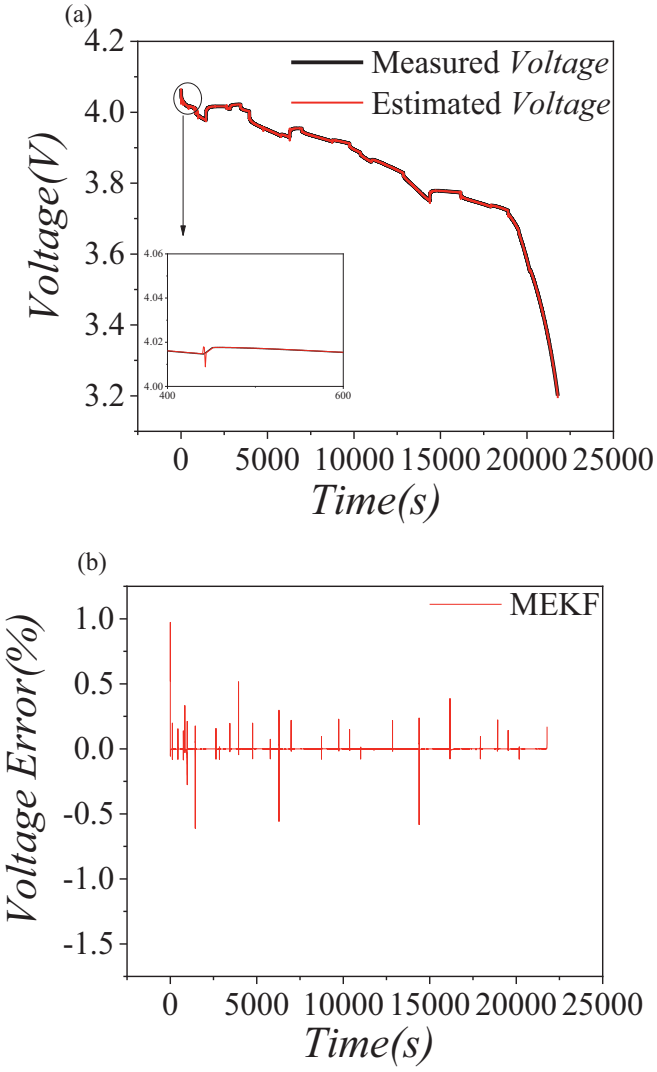

Fig. 8. (a) Comparison of measured and estimated voltages using the MEKF algorithm under the current pattern in Fig. 5(a), and the corresponding error.

$$y_k = \boldsymbol{C}_k x_k + \boldsymbol{D}_{\mathbf{k}} u_{\mathrm{k}} + v_k \tag{7}$$

where x_k is a column vector with the states of the system, $\boldsymbol{A}_{\mathbf{k}}$ is the system dynamics matrix, u_k is the control vector, $\boldsymbol{B}_{\mathbf{k}}$ is the control matrix, w_k is a white-noise vector. y_k is a measurement vector, $\boldsymbol{C}_{\mathbf{k}}$ is the measurement matrix, Q_k is the system noise matrix, and v_k is the measurement noise.

The following equations can be acquired based on (6) and (7):

$$x_{k+1} = \mathrm{f}(x_k, u_k) + \boldsymbol{\Gamma}_{\mathbf{k}} w_k \tag{8}$$

$$\mathrm{y}_{\mathrm{k}} = \mathrm{g}(x_k, u_k) + v_k \tag{9}$$

where $f(x_k, u_k)$ is a non-linear state transition function, $g(x_k, u_k)$ is a non-linear state measurement function. $f(x_k, u_k)$ and $g(x_k, u_k)$ are linearized according to the first-order Taylor expansion at each point in time. All sampling points are assumed to be differentiable.

$\overline{\boldsymbol{A}}_{\mathbf{k}} = \frac{\partial \mathrm{f}(x_k, u_k)}{\partial x_k}\Big|_{x_k = \overline{x}_k}$, $\overline{\boldsymbol{C}}_{\mathrm{k}} = \frac{\partial \mathrm{g}(x_k, u_k)}{\partial x_k}\Big|_{x_k = \overline{x}_k}$, expressions related to the state vector can be derived by Eqs. (6) and (7).

$$x_{k+1} \approx \overline{\boldsymbol{A}}_{\mathbf{k}} x_k + [\mathrm{f}(\overline{x}_k, u_k) - \overline{\boldsymbol{A}}_{\mathbf{k}} \overline{x}_k] + \boldsymbol{\Gamma}_{\mathbf{k}} w_k \tag{10}$$

$$\mathrm{y}_{\mathrm{k}} \approx \overline{\boldsymbol{C}}_{\mathbf{k}} x_k + [g(\overline{x}_k, u_k) - \overline{\boldsymbol{C}}_{\mathbf{k}} \overline{x}_k] + v_k \tag{11}$$

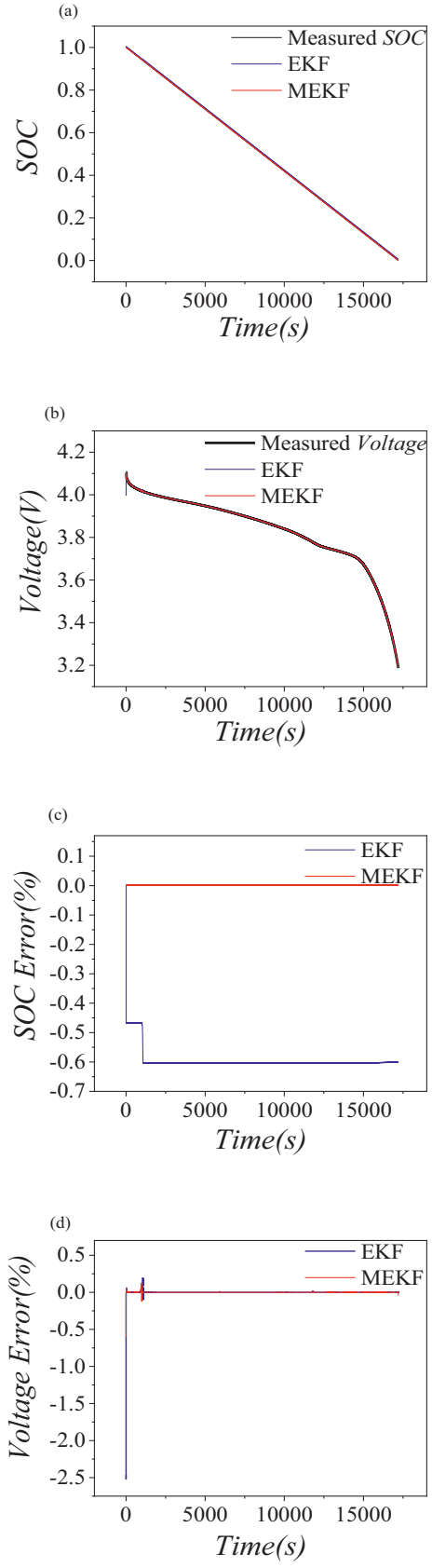

Fig. 9. Comparison of measured and estimated (a) *SOC*s and (b) voltages using the EKF and MEKF algorithms, and (c, d) their corresponding errors.

The process of the MEKF algorithm for non-linear systems can be presented by the following formulas.

The update of the status matrix:

$$x_{k/k-1} = \mathrm{f}\left(\bar{x}_{k-1/k-1}, u_{k-1}\right) \tag{12}$$

The update of the covariance matrix:

$$P_{k/k-1} = \boldsymbol{A_{k-1}} P_{k-1/k-1} \boldsymbol{A_{k-1}^{T}} + \boldsymbol{\Gamma_{k-1}} Q_{l(k-1)} \boldsymbol{\Gamma_{k-1}^{T}} \tag{13}$$

The Kalman gains matrix:

$$K_k = P_{k/k-1} \boldsymbol{C_{k-1}^{T}} \left(\boldsymbol{C_k} P_{k/k-1} \boldsymbol{C_k^{T}} + R_{l(k)}\right)^{-1} \tag{14}$$

The Kalman gains matrix adjustment by current detecting:

$$\boldsymbol{K_k} = \boldsymbol{T_k} \boldsymbol{K_{k-1}} \tag{15}$$

The measurement update of the status matrix:

$$\bar{x}_{k/k} = \bar{x}_{k/k-1} + \boldsymbol{K_k}\left(\mathrm{y_k} - \boldsymbol{C_k}^{'} \bar{x}_{k/k-1} - \boldsymbol{D_k} u_k\right) \tag{16}$$

The measurement update of the covariance matrix:

$$P_{k/k} = (\boldsymbol{I} - \boldsymbol{K_k} \boldsymbol{C_k}^{'}) P_{k/k-1} \tag{17}$$

The estimation formula of the output vector is:

$$\hat{y}_{\mathrm{k}} = g\left(\bar{x}_{k/k-1}, u_k\right) \tag{18}$$

where $x_{\mathrm{k/k-1}}$ is the forecast value of status, $x_{\mathrm{k/k}}$ is the filtering value of status, K_k is the Kalman filtering gains matrix, $P_{k/k}$ is the value of the filtering covariance matrix, $P_{k/k-1}$ is the forecast covariance matrix, $Q_{l(k-1)}$ is the process noise, $R_{l(k)}$ is the measurement noise, and I is the unit matrix. $\overline{\boldsymbol{A}}_{\mathbf{k}}$ and $\overline{\boldsymbol{C}}_{\mathbf{k}}^{'}$ are calculated by the linearization of the model.

Unknown measurement noise and system noise are the key factors that affect the estimation accuracy of voltage and *SOC* through the EKF method [37]. Accurate noise estimation is essential to reduce the influence of noises in the estimation process. Different from the traditional method of setting the noise through the given parameters of the equipment, the MEKF algorithm is to set and adjusts the measurement noise through the voltage error generated during the estimation process. The strength of our proposed method is that unmeasurable noises such as ambient noise could also be incorporated into the estimation of measurement noise, which can realize the simple and targeted measurement noise prediction. A diagonal matrix is built based on the values of measurement noise obtained as Eq. (19), which is used for the estimation of the process noise. The errors induced by discretization and linearization of the model, and the round-off error can be reduced by the adjustment matrix $\boldsymbol{M_l}$.

$$R_l = H_l V_{MinE} \tag{19}$$

$$\boldsymbol{Q_l} = R_l \boldsymbol{I} \boldsymbol{M_l} \tag{20}$$

$$\boldsymbol{M_l} = \begin{bmatrix} 1000 & 0 & 0 \\ 0 & 10 & 0 \\ 0 & 0 & 0.1 \end{bmatrix} \tag{21}$$

Besides, the observation matrix $\boldsymbol{C_k}^{'}$ in the MEKF algorithm is different from $\boldsymbol{C_k}$ in the traditional EKF algorithm, which is shown in the following equations:

$$\boldsymbol{C_k}^{'} = \frac{\partial U_l}{\partial X} = \left[\frac{\partial U_1}{\partial U_p} \quad \frac{\partial U_2}{\partial U_p} \quad \frac{\partial U_L^{n+1}}{\partial SOC}\right] \tag{22}$$

$$\frac{\partial U_L^{n+1}}{\partial SOC} = \frac{\partial U_{OC}^{n+1}}{\partial SOC} + \frac{\partial R_0^{n+1}}{\partial SOC} \tag{23}$$

where U_L^{n+1} is the loading voltage in Fig. 1, and $n+1$ is the curve fitting order between the U_L and *SOC*. Eqs. (22) and (23) are adopted as the observation matrix in the MEKF, while the fitting order of U_{OC}^{n} and R_0^{n} are

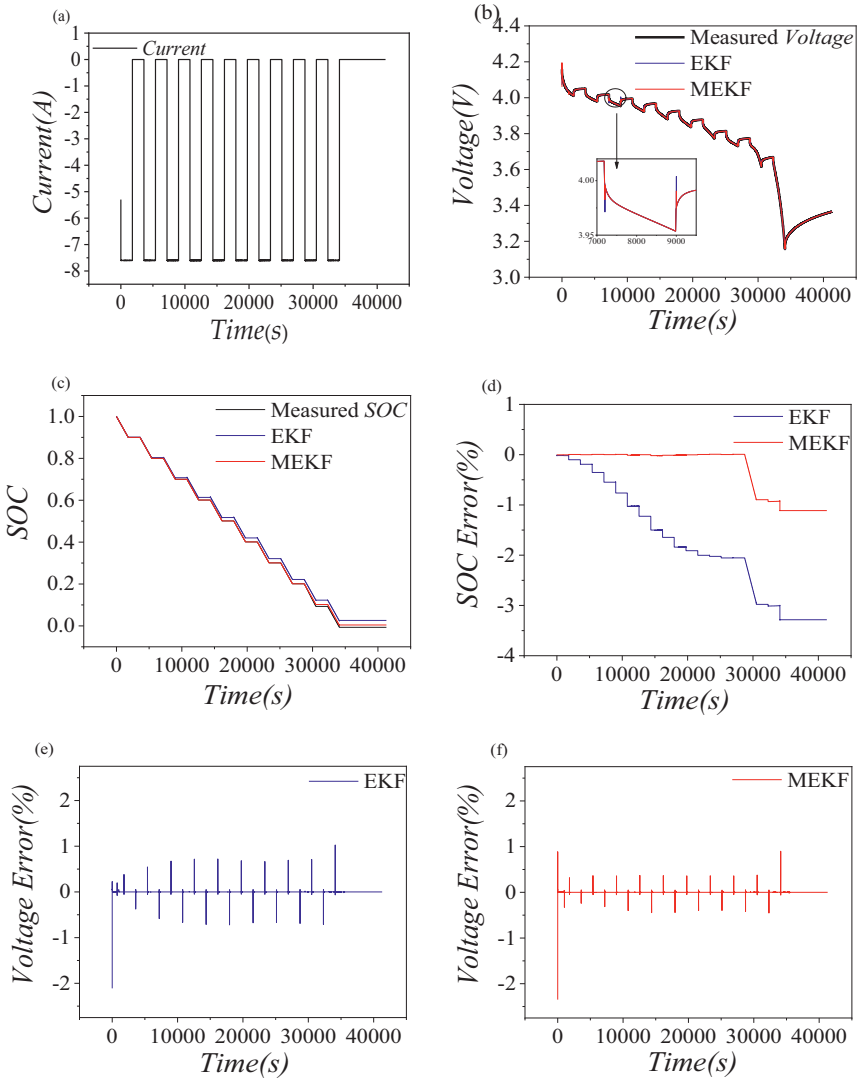

Fig. 10. (a) Testing condition: the applied current of the pulse discharge; Comparisons of measured and estimated (b) voltages and (c) *SOC*s using the EKF and MEKF algorithms, and (d–f) their corresponding errors, respectively.

applied simultaneously. As errors would be induced when the observation matrix is applied according to the measurement noise and equation linearization [43], the higher fitting order of the observation matrix is desired. The observation matrix $\boldsymbol{C_k}'$ is used to enhance the *SOC* estimation accuracy in Eq. (16). where x_k is a column vector with the states of the system, u_k is a known vector (also called a control vector), $\boldsymbol{K_k}$ is the Kalman gain matrix, and D_k is a random variable.

The MEKF algorithm adopts noise adjustment and DBOFT to reduce the influence of noises on voltage and *SOC* estimations. The Kalman gain matrix (shown in Eq. (1)) is used to reduce the error of voltage estimation, especially at each turning point of current. Finally, the optimal parameters for the voltage and *SOC* estimations could be obtained along with the flow chart as shown in Fig. 3.

In this study, a 38 Ah YUASA LEV50 cell with a discharged capacity of 38 Ah is employed as a rechargeable battery to verify the MEKF algorithm for voltage and *SOC* estimations [44]. Specifically, the Kalman gain and noise are studied for the estimation of battery voltage. The approaches to designing the Kalman gain and voltage estimation at the turning points of current would effectively reduce the errors of estimated voltage and *SOC*. The MEKF algorithm is also validated effectively with a designated working current.

4. Results and discussion

4.1. Parameter identification and data acquisition

The offline parameter identification was carried out using a high-precision multimeter (Keithley 2002) to ensure the accuracy of the battery model. The cell was discharged at 0.2C for half an hour and then hold for half an hour to reach an equilibrium state. The voltage was detected by the multimeter during the discharge process. The process was repeated 10 times under an ambient temperature of 298 K. The offline parameter identification results are shown in Table 1.

To verify the accuracy of the parameters to the physical model, the derived data in Table 1 were simulated by Simulink. Fig. 4 shows that the second-order battery model can be well modeled for the actual LIBs. In Fig. 4(b), the error between the simulated and the measured voltage is within 1 % except for the abrupt change at the end due to the degrading activity of graphite (R_0 increases at the end of discharging) [45–47]. This is also consistent with our R_0 value as shown in Table 1.

4.2. Voltage estimation accuracy improvement

Fig. 5(a) shows the current applied to the battery while Fig. 5(b) compares the measured voltage with the estimation using the EKF

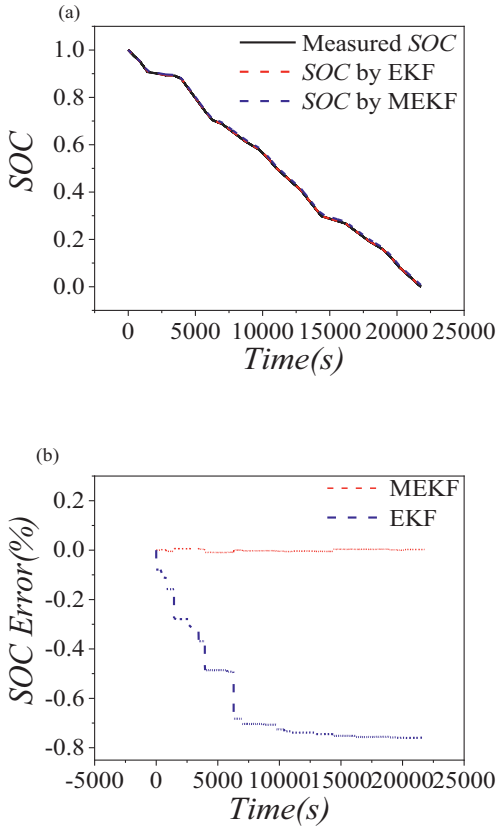

Fig. 11. Comparison of (a) measured and estimated *SOC*s using the EKF and MEKF algorithms under the current pattern in Fig. 5(a), and (b) their corresponding errors.

algorithm. It can be seen that errors between the measurement and estimation are significant, especially at the sudden changes in current. The maximum estimation error was 1.386 %. To investigate and confirm the origin of errors, a regular pattern of electric current was designed as shown in Fig. 6. Fig. 7(a) shows that the voltage estimated using the EKF algorithm agreed well with the measured values except at the instantaneous transition from minimum to maximum, or vice versa. As the sharp turning points of the current could be identified and recorded following the noise and K_k adjustments using the MEKF algorithm, the estimated voltage error was reduced significantly even at the instantaneous transitions as shown in Fig. 7.

To further demonstrate the capability of voltage estimation, the MEKF algorithm was employed to simulate the voltage with the irregular current pattern in Fig. 5(a). Fig. 8 shows that the voltage estimation error was still greatly reduced even though the current pattern was non-periodic with many instantaneous changes. When compared to the EKF algorithm (Fig. 5(c)), the MEKF algorithm could offer much higher accuracy (Fig. 8(b)), which reduced the maximum voltage estimation error and the average estimation error to 0.972 % and 0.000001 %, respectively.

4.3. SOC estimation accuracy improvement

Fig. 9(a) and (b) show the measured and estimated *SOC*s and the corresponding errors induced by the conventional EKF and MEKF algorithms, respectively. It was found that the MEKF algorithm induced much smaller errors in *SOC* estimation when compared to the conventional EKF algorithm. By using the MEKF algorithm, the maximum *SOC* estimation error was reduced from 0.6032 % to 0.0052 %, which is attributed to the proposed continuous parameters optimization and data analysis during iteration. The maximum estimated voltage error was also reduced from 2.5182 % into 0.5995 % as shown in Fig. 9(c) and (d).

The performance of the MEKF algorithm was further evaluated with the regular pulse discharge mode as shown in Fig. 10(a). Fig. 10(b) and (c) compare the voltage and *SOC* acquired from the measurements and both the EKF and MEKF algorithms, respectively, while Fig. 10(d) to (f) show the errors induced by algorithms. The maximum *SOC* error was reduced from 3.2844 % to 1.1121 % by using the MEKF algorithm as shown in Fig. 10(d). Similarly, the estimated voltage errors using the MEKF algorithm were reduced significantly when compared to the ones induced by the conventional algorithm.

Besides the periodic current pattern, the MEKF algorithm was tested under the irregular current condition as shown in Fig. 5(a). Fig. 11 shows the comparison of the measured and estimated *SOC*s using the EKF and MEKF algorithms. The error induced by the MEKF algorithm was very small when compared to those using the conventional EKF algorithm (0.7589 %), which was reduced to 0.01016 % as shown in Fig. 11(b). To verify the feasibility, the MEKF algorithm was applied on the battery with the lower capacity under more complex current conditions (0.00015C to 0.55C) as shown in Fig. 12(a). It was found that the MEKF could reduce the voltage error at the current changing points and enhance the *SOC* estimation accuracy as shown in Figs. 5(a) and 12(a), respectively.

Table 2 shows the comparison of both *SOC* and voltage estimation errors between the proposed MEKF algorithm and other reported work. The MEKF algorithm exhibits the highest accuracy on both *SOC* and voltage estimations, in which the errors are much smaller. The results proved that the proposed MEKF algorithm is promising for practical battery monitoring under any current situation, for example, the precise voltage estimation can be applied to monitor if the battery voltage exceeds the safe voltage level [48,49].

To investigate the effect on the computational complexity of the MEKF, the EKF and MEKF were run for 50 times through Matlab and the CPU times were recorded for the high-power and low-power LIBs, respectively, as shown in Fig. 13. According to the data analysis in Table 3, the average CPU runtime of the MEKF is 6.71117 s, which is slightly longer than that of the EKF (6.63812 s). Since the amount of data in the high-power LIB is much more than that in the low-power LIB, the runtime for the high-power LIB would be longer.

Based on the results, the MEKF increased the computational load but within an acceptable range. The modification focused on the matrix adjustment of the original core formula, while the algorithm load was mainly induced from the DBOFT and current mutation point detection. As external factors such as signal transmission delay of the sensor were not taken into account, the MEKF still needs to be tested extensively and adjusted for continuous improvement in real applications.

5. Conclusion

Battery safety is crucial for applications such as EVs, in which many aspects such as *SOC*, current, and voltage are required to be simultaneously monitored. Accurate *SOC* estimation allows the battery to distribute energy effectively and operate safely. As battery current monitoring can be very complicated, accurate voltage estimation is highly desired in terms of simplicity and accuracy for battery health monitoring. The effectiveness of adjustment on the factors such as noise and Kalman gain is critical for providing an accurate battery performance estimation.

The proposed MEKF algorithm, based on the conventional EKF, is developed to improve the accuracy of voltage and *SOC* estimations for rechargeable batteries. This work explores the approaches to minimize the errors in voltage and *SOC* estimations for high- and low-power LIBs, respectively. The DBOFT is also proposed to automatically determine the optimal fitting order for building a mathematical model to describe the characteristics of batteries.

The main contribution of the work is to improve the accuracy of voltage and *SOC* estimations via matrix and noise correction techniques

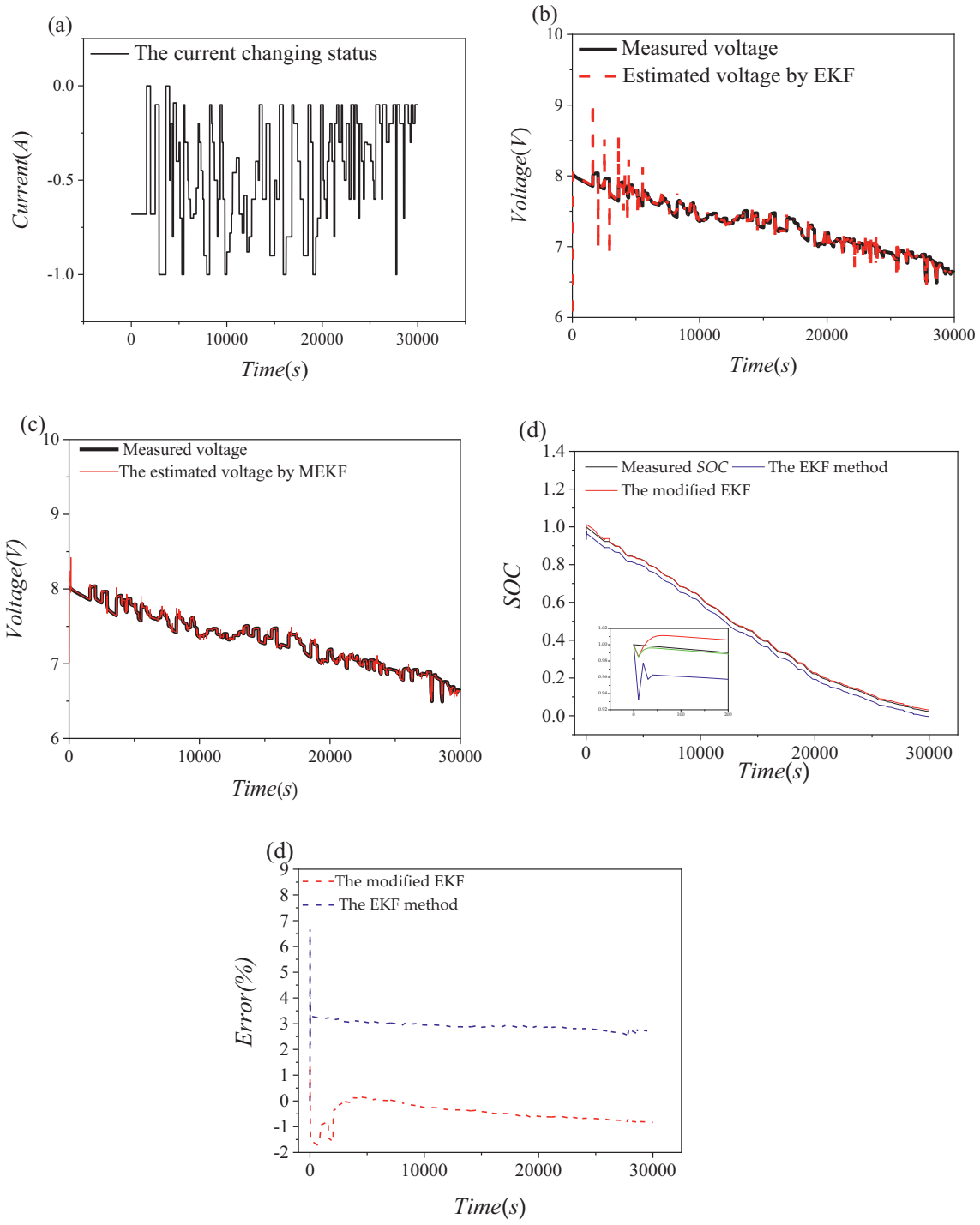

Fig. 12. Comparison between measured and estimated (a) Irregular current pattern applied to the battery with the capacity of 3.4 Ah (b) voltages using the EKF and (c) MEKF, (d) SOC using the EKF and MEKF, and (e) corresponding SOC errors for a battery with the capacity of 3.4 Ah under the discharging current condition in Fig. 12(a).

especially at the current changing points for the first time. Besides, with using the DBOFT, the errors in battery modeling are also reduced, which is crucial for battery status monitoring. Most importantly, the approach adopted in MEKF is based on the error adjustment function of Kalman gain and therefore can be applied with other Kalman-based algorithms.

Nevertheless, when compared to online parameter identification, the offline parameter identification method adopted in this work cannot reflect the internal changes of the battery in real-time through the battery model. In the near future work, the focus will be on the integration of online parameter identification with MEKF for *SOC* estimation incorporating more real-time impact factors. In addition, factors such as temperature and battery aging will be considered in *SOC* estimation by neural network models. *SOC* estimation by artificial intelligence (AI) approaches such as machine learning will also be the main research pathway in the future.

Table 2
Comparison of *SOC* and voltage estimation errors between the MEKF and reported work.

Method	Maximum *SOC* error (constant current discharge test)	Maximum *SOC* error (irregular current test)	Maximum voltage error (irregular current test)
Parameter adaptive method [39]	1.43 %	2.94 %	12.14 %
SOC estimation method [50]	/	2 %	5.95 %
Online *SOC* and capacity estimation method [51]	/	5 %	/
Energy management strategy [52]	/	2.2 %	1.92 %
Charged state prediction method [18]	/	1.38 %	9.2 %
SOC estimation method [53]	/	15 %	5.5 %
Improved *SOC* estimation method [54]		2 %	2.8 %
SOC estimation of batteries [36]	/	2 %	1.3 %
EKF based on temperature-compensated model [55]	3 %	1.5 %	2.5 %
Adaptive fading-extended Kalman filter [56]	/	2.6 %	2.28 %
MEKF	0.0052 %	0.01016 %	0.972 %

Notations

R_0	Battery ohmic internal resistance (Ω)
R_1	Electrochemical polarization internal resistance (Ω)
R_2	Consistence polarize internal resistance (Ω)
C_1	Electrochemical polarization capacitor (*F*)
C_2	Consistence polarize internal resistance (*F*)
U_{OC}	The open-circuit-voltage of the battery (*V*)
U_L	The terminal voltage of the battery (*V*)
U_1	Electrochemical polarization circuit voltage of the battery (*V*)
U_2	Consistence polarization circuit voltage of the battery (*V*)
I_k	Battery current
V_{MinE}	Minimum voltage error between simulated voltage and measured voltage (*V*)
$\boldsymbol{O}_{mn}$	Polynomial fitting parameters matrix
V_n	Polynomial fitting parameters
S_{nm}	Essential matrix consisting of *SOC*
$\boldsymbol{M}_{mm}$	Mathematical battery model
$\boldsymbol{T_k}$	Adjustment matrix of Kalman gain
z	Measurement noise adjustment parameter based on the maximum voltage estimation error
P_k	Covariance matrix
$\boldsymbol{A_k}$	System dynamics matrix
$\boldsymbol{B_k}$	Control matrix
$\boldsymbol{C_k}$	Observation matrix in the conventional EKF
$\boldsymbol{C_k}'$	Observation matrix in the MEKF
$\boldsymbol{K_k}$	Kalman gain matrix
R	Covariance matrix of the measurement noise
Q	Covariance matrix of the process noise
$\boldsymbol{I}$	Unit diagonal matrix
$\boldsymbol{M_l}$	The adjustment matrix of the process noise
x_k	A column vector with the states of the system
y_k	A measurement vector

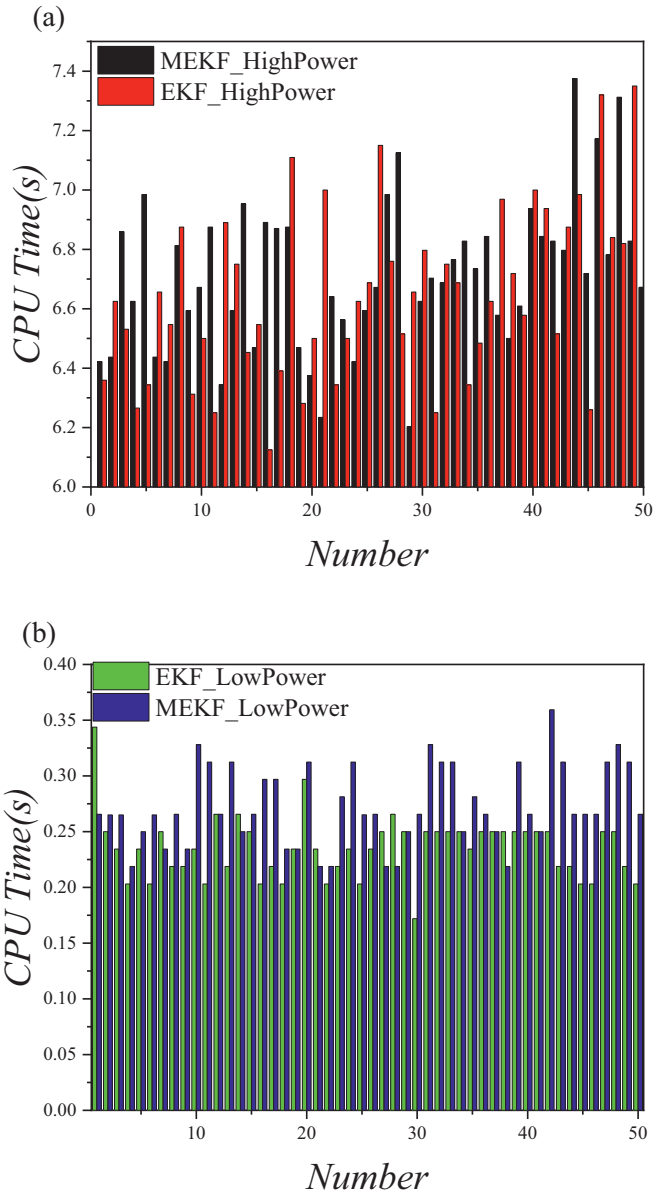

Fig. 13. Comparison of CPU runtime between employing MEKF and EKF algorithms on (a) a high-power LIB with the capacity of 38 Ah, and (b) a low-power LIB with the capacity of 3.4 Ah.

Table 3
Comparison of statistical analysis for CPU runtime between the MEKF and EKF.

Approach	Mean (*s*)	Maximum (*s*)	Standard deviation
CPU time of MEKF (high-power)	6.71117	7.375	0.25125
CPU time of EKF (high-power)	6.63812	7.35	0.29171
CPU time of MEKF (low-power)	0.27246	0.3594	0.03532
CPU time of EKF (low-power)	0.23532	0.3438	0.02814

w_k	A white-noise vector
v_k	The measurement noise vector

Credit authorship contribution statement

Fan YANG: Writing-Original draft preparation. **Fan YANG**, **Dongliang SHI**: Methodology, Software, Data curation **Dongliang SHI**:

Visualization, Investigation. **Kwok-ho LAM**: Conceptualization **Kwok-ho LAM**: Supervision. **Fan YANG**: Validation. **Fan YANG, Dongliang SHI, Kwok-ho LAM**: Writing- Reviewing and Editing.

Declaration of competing interest

All co-authors have seen and agreed with the content of the manuscript and there is no financial interest to report. We declare that the manuscript is original, which has not been published before or submitted elsewhere for the consideration of publication. We know of no conflicts of interest associated with this work, and there has been no significant financial support for this work that could have influenced its outcome.

Data availability

Data will be made available on request.

Acknowledgments

This work was supported financially by the Hong Kong Polytechnic University and the University of Glasgow.

References

[1] İ.A. Reşitoğlu, K. Altinişik, A. Keskin, The pollutant emissions from diesel-engine vehicles and exhaust aftertreatment systems, Clean Techn. Environ. Policy 17 (1) (2015) 15–27, https://doi.org/10.1007/s10098-014-0793-9.
[2] X. Chen, et al., A novel approach to reconstruct open circuit voltage for state of charge estimation of lithium ion batteries in electric vehicles, Appl. Energy 255 (2019), 113758, https://doi.org/10.1016/j.apenergy.2019.113758.
[3] P. Iurilli, C. Brivio, M. Merlo, SoC management strategies in battery energy storage system providing primary control reserve, Sustain. Energy, Grids Netw. 19 (2019), 100230, https://doi.org/10.1016/j.segan.2019.100230.
[4] J.H. Aylor, A. Thieme, B.W. Johnso, A battery state-of-charge indicator for electric wheelchairs, IEEE Trans. Ind. Electron. 39 (5) (1992) 398–409, https://doi.org/10.1109/41.161471.
[5] S. Pang, et al., Battery state-of-charge estimation, in: Proceedings of the 2001 American Control Conference (Cat. No. 01CH37148), IEEE, 2001, https://doi.org/10.1109/ACC.2001.945964.
[6] G.L. Plett, Kalman-filter SOC estimation for LiPB HEV cells, in: Proceedings of the 19th International Battery, Hybrid and Fuel Cell Electric Vehicle Symposium & Exhibition (EVS19), 2002, pp. 527–538, 10.1.1.630.7523.
[7] L. Kang, X. Zhao, J.J.A.E. Ma, A New Neural Network Model for the State-of-charge Estimation in the Battery Degradation Process 121, 2014, pp. 20–27, https://doi.org/10.1016/j.apenergy.2014.01.066.
[8] C. Cai, D. Du, Z. Liu, Battery state-of-charge (SOC) estimation using adaptive neuro-fuzzy inference system (ANFIS), in: The 12th IEEE International Conference on Fuzzy Systems (FUZZ'03) 2, IEEE, 2003, pp. 1068–1073, https://doi.org/10.1109/FUZZ.2003.1206580.
[9] H. Dai, et al., Online cell SOC estimation of Li-ion battery packs using a dual time-scale Kalman filtering for EV applications, Appl. Energy 95 (2012) 227–237, https://doi.org/10.1016/j.apenergy.2012.02.044.
[10] Z. Deng, et al., Data-driven state of charge estimation for lithium-ion battery packs based on Gaussian process regression, Energy 205 (2020), 118000, https://doi.org/10.1016/j.energy.2020.118000.
[11] S. Li, et al., Lithium-ion battery modeling based on Big Data, Energy Procedia 159 (2019) 168–173, https://doi.org/10.1016/j.egypro.2018.12.046.
[12] K.P. Guodong Fan, Marcello Canova, A comparison of model order reduction techniques for electrochemical characterization of lithium-ion batteries, in: IEEE 54th Annual Conference on Decision and Control (CDC), 2015, pp. 3922–3931, https://doi.org/10.1109/CDC.2015.7402829.
[13] H. He, R. Xiong, J. Fan, Evaluation of lithium-ion battery equivalent circuit models for state of charge estimation by an experimental approach, Energies 4 (2011) 582–598, https://doi.org/10.3390/en4040582.
[14] X. Dang, et al., Open-circuit voltage-based state of charge estimation of lithium-ion battery using dual neural network fusion battery model, Electrochim. Acta 188 (2016) 356–366, https://doi.org/10.1016/j.electacta.2015.12.001.
[15] J.B. Robinson, et al., Spatially resolved ultrasound diagnostics of Li-ion battery electrodes, Phys. Chem. Chem. Phys. 21 (2019) 6354–6361, https://doi.org/10.1039/C8CP07098A.
[16] J.J. Chang, X.F. Zeng, T.L. Wan, Real-time measurement of lithium-ion batteries' state-of-charge based on air-coupled ultrasound, AIP Adv. 9 (8) (2019), 085116, https://doi.org/10.1063/1.5108873.
[17] S.L. Wang, et al., An improved coulomb counting method based on dual open-circuit voltage and real-time evaluation of battery dischargeable capacity considering temperature and battery aging, Int. J. Energy Res. 45 (12) (2021) 17609–17621, https://doi.org/10.1002/er.7042.
[18] S. Wang, et al., A novel charged state prediction method of the lithium ion battery packs based on the composite equivalent modeling and improved splice Kalman filtering algorithm, J. Power Sources 471 (2020), 228450, https://doi.org/10.1016/j.jpowsour.2020.228450.
[19] M. Charkhgard, M. Farrokhi, State-of-charge estimation for lithium-ion batteries using neural networks and EKF, IEEE Trans. Ind. Electron. 57 (12) (2010) 4178–4187, https://doi.org/10.1109/TIE.2010.2043035.
[20] Y. Qiu, et al., State of charge estimation of vanadium redox battery based on improved extended Kalman filter, ISA Trans. 94 (2019) 326–337, https://doi.org/10.1016/j.isatra.2019.04.008.
[21] G.L.J.J.o.P.s. Plett, Extended Kalman filtering for battery management systems of LiPB-based HEV battery packs: part 3. State and parameter estimation, J. Power Sources 134 (2) (2004) 277–292, https://doi.org/10.1016/j.jpowsour.2004.02.033.
[22] A. Vasebi, M. Partovibakhsh, S.M.T. Bathaee, A novel combined battery model for state-of-charge estimation in lead-acid batteries based on extended Kalman filter for hybrid electric vehicle applications, J. Power Sources 174 (1) (2007) 30–40, https://doi.org/10.1016/j.jpowsour.2007.04.011.
[23] N. Wassiliadis, et al., Revisiting the dual extended Kalman filter for battery state-of-charge and state-of-health estimation: a use-case life cycle analysis, J. Energy Storage 19 (2018) 73–87, https://doi.org/10.1016/j.est.2018.07.006.
[24] L. Xia, et al., Joint estimation of the state-of-energy and state-of-charge of lithium-ion batteries under a wide temperature range based on the fusion modeling and online parameter prediction, J. Energy Storage 52 (2022), 105010, https://doi.org/10.1016/j.est.2022.105010.
[25] C. Campestrini, et al., A comparative study and review of different Kalman filters by applying an enhanced validation method, J. Energy Storage 8 (2016) 142–159, https://doi.org/10.1016/j.est.2016.10.004.
[26] H. Dai, et al., Online cell SOC estimation of Li-ion battery packs using a dual time-scale Kalman filtering for EV applications, Appl. Energy 95 (2012) 227–237, https://doi.org/10.1016/j.apenergy.2012.02.044.
[27] H. He, et al., State-of-charge estimation of the lithium-ion battery using an adaptive extended Kalman filter based on an improved Thevenin model, IEEE Trans. Veh. Technol. 60 (4) (2011) 1461–1469, https://doi.org/10.1109/TVT.2011.2132812.
[28] M. Dahmardeh, Z.J.J.o.E.S. Xi, Probabilistic state-of-charge estimation of lithium-ion batteries considering cell-to-cell variability due to manufacturing tolerance, J. Energy Storage 43 (2021), 103204, https://doi.org/10.1016/j.est.2021.103204.
[29] Z. Wei, et al., Load current and state-of-charge coestimation for current sensor-free lithium-ion battery, IEEE Trans. Power Electron. 36 (10) (2021) 10970–10975, https://doi.org/10.1109/TPEL.2021.3068725.
[30] L.-L. Li, et al., Improved tunicate swarm algorithm: solving the dynamic economic emission dispatch problems, Appl. Soft Comput. 108 (2021), 107504, https://doi.org/10.1016/j.asoc.2021.107504.
[31] Z.-F. Liu, et al., Dynamic economic emission dispatch considering renewable energy generation: a novel multi-objective optimization approach, Energy 235 (2021), 121407, https://doi.org/10.1016/j.energy.2021.121407.
[32] D. Liu, A novel fading memory recursive least square method (FMLS) for accurate state of charge estimation of lithium- ion batteries combined with improved second order PNGV modeling, Int. J. Electrochem. Sci. 16 (9) (2021), https://doi.org/10.20964/2021.09.34.
[33] A. Seaman, T.-S. Dao, J. McPhee, A survey of mathematics-based equivalent-circuit and electrochemical battery models for hybrid and electric vehicle simulation, J. Power Sources 256 (2014) 410–423, https://doi.org/10.1016/j.jpowsour.2014.01.057.
[34] B. Rzepka, S. Bischof, T. Blank, Implementing an extended Kalman filter for SoC estimation of a Li-ion battery with hysteresis: a step-by-step guide, Energies 14 (13) (2021) 3733, https://doi.org/10.3390/en14133733.
[35] L. Guo, J. Li, Z. Fu, Lithium-ion battery SOC estimation and hardware-in-the-loop simulation based on EKF, Energy Procedia 158 (2019) 2599–2604, https://doi.org/10.1016/j.egypro.2019.02.009.
[36] R. Xiong, et al., Evaluation on state of charge estimation of batteries with adaptive extended Kalman filter by experiment approach, IEEE Trans. Veh. Technol. 62 (1) (2013) 108–117, https://doi.org/10.1109/TVT.2012.2222684.
[37] W. Kai, State of charge (SOC) estimation of lithium-ion battery based on adaptive square root unscented Kalman filter, Int. J. Electrochem. Sci. 15 (9) (2020) 9499–9516, https://doi.org/10.20964/2020.09.84.
[38] K. Yang, Y. Tang, Z. Zhang, Parameter identification and state-of-charge estimation for lithium-ion batteries using separated time scales and extended Kalman filter, Energies 14 (4) (2021) 1054, https://doi.org/10.3390/en14041054.
[39] S. Yang, et al., A parameter adaptive method for state of charge estimation of lithium-ion batteries with an improved extended Kalman filter, Sci. Rep. 11 (1) (2021) 1–15, https://doi.org/10.1038/s41598-021-84729-1.
[40] P. Zarchan, Fundamentals of Kalman Filtering: A Practical Approach, AIAA, 2009.
[41] J. Lee, O. Nam, B.H. Cho, Li-ion battery SOC estimation method based on the reduced order extended Kalman filtering, J. Power Sources 174 (1) (2007) 9–15, https://doi.org/10.1016/j.jpowsour.2007.03.072.
[42] Y. Li, C. Wang, J. Gong, A combination Kalman filter approach for state of charge estimation of lithium-ion battery considering model uncertainty, Energy 109 (2016) 933–946, https://doi.org/10.1016/j.energy.2016.05.047.
[43] H. Durrant-Whyte, Introduction to Estimation and the Kalman Filter, Australian Centre for Field Robotics, 2001.
[44] Ryan C. Kroeze, P.T. K., Electrical battery model for use in dynamic electric vehicle simulations, in: IEEE Power Electronics Specialists Conference, 2008, pp. 1336–1342, https://doi.org/10.1109/PESC.2008.4592119.

[45] L. Zhang, et al., Comparative research on RC equivalent circuit models for lithium-ion batteries of electric vehicles, Appl. Sci. 7 (10) (2017), https://doi.org/10.3390/app7101002.
[46] Q. Wang, et al., Correlation between the model accuracy and model-based SOC estimation, Electrochim. Acta 228 (2017) 146–159, https://doi.org/10.1016/j.electacta.2017.01.057.
[47] O. Tremblay, L.-A. Dessaint, A.-I. Dekkiche, A generic battery model for the dynamic simulation of hybrid electric vehicles, in: IEEE Vehicle Power and Propulsion Conference, 2007, pp. 284–289, https://doi.org/10.1109/VPPC.2007.4544139.
[48] A.B. Lopez, et al., A security perspective on battery systems of the internet of things, J. Hardw. Syst. Secur. 1 (2) (2017) 188–199, https://doi.org/10.1007/s41635-017-0007-0.
[49] S.M. Rezvanizaniani, et al., Review and recent advances in battery health monitoring and prognostics technologies for electric vehicle (EV) safety and mobility, J. Power Sources 256 (2014) 110–124, https://doi.org/10.1016/j.jpowsour.2014.01.085.
[50] C. Jiang, et al., A state-of-charge estimation method of the power lithium-ion battery in complex conditions based on adaptive square root extended Kalman filter, Energy 219 (2021), https://doi.org/10.1016/j.energy.2020.119603.
[51] C. Yang, et al., An online SOC and capacity estimation method for aged lithium-ion battery pack considering cell inconsistency, J. Energy Storage 29 (2020), https://doi.org/10.1016/j.est.2020.101250.
[52] S. Wang, et al., A novel energy management strategy for the ternary lithium batteries based on the dynamic equivalent circuit modeling and differential Kalman filtering under time-varying conditions, J. Power Sources 450 (2020), https://doi.org/10.1016/j.jpowsour.2019.227652.
[53] Q. Zhu, et al., A state of charge estimation method for lithium-ion batteries based on fractional order adaptive extended kalman filter, Energy 187 (2019), https://doi.org/10.1016/j.energy.2019.115880.
[54] J. Peng, et al., An improved state of charge estimation method based on cubature Kalman filter for lithium-ion batteries, Appl. Energy 253 (2019), https://doi.org/10.1016/j.apenergy.2019.113520.
[55] K. Lee, M. D., C. Chuang, Temperature-compensated model for lithium-ion polymer batteries with extended Kalman filter state-of-charge estimation for an implantable charger, IEEE Trans. Ind. Electron. 65 (2018) 589–596, https://doi.org/10.1109/TIE.2017.2721880.
[56] P. Takyi-Aninakwa, et al., A strong tracking adaptive fading-extended Kalman filter for the state of charge estimation of lithium-ion batteries, Int. J. Energy Res. (2022), https://doi.org/10.1002/er.8307.